JACS
JOURNAL OF THE AMERICAN CHEMICAL SOCIETY
COMMUNICATION
pubs.acs.org/JACS

Molecular Lithography through DNA-Mediated Etching and Masking of SiO_2

Sumedh P. Surwade,[†,§] Shichao Zhao,[†,‡,§] and Haitao Liu*[,†]

[†]Department of Chemistry, University of Pittsburgh, Pittsburgh, Pennsylvania 15260, United States
[‡]College of Materials & Environmental Engineering, Hangzhou Dianzi University, Hangzhou 310018, P. R. China

S Supporting Information

ABSTRACT: We demonstrate a new approach to pattern transfer for bottom-up nanofabrication. We show that DNA promotes/inhibits the etching of SiO_2 at the single-molecule level, resulting in negative/positive tone pattern transfers from DNA to the SiO_2 substrate.

State-of-the-art photolithography processes use 193 nm light to produce diffraction-limited features as small as 32 nm.[1] The use of even shorter wavelengths of light faces significant technological and economic challenges because of the cost and complexity of the exposure optics and the high-energy light source. Thus, over the past few years, significant efforts have been dedicated toward alternative lithography processes that can produce features with sizes in the range of tens of nanometers.

In recent years, self-assembly of DNA, especially of scaffolded DNA origami, has matured to a stage where arbitrary two- and three-dimensional shapes with controlled dimensions at the nanoscale can easily be constructed.[2,3] These DNA nanostructures have been used to direct the assembly of nanoparticles, carbon nanotubes, and biological molecules.[4−15] With a patterned substrate, they can be deposited with precise control over their location and orientation, opening up the possibility that they can be fully integrated with conventional lithography processes.[5,14,16,17]

In view of the degree of control over their sizes and shapes, these DNA nanostructures should be ideal templates for bottom-up nanofabrication. Unfortunately, DNA nanostructures have limited chemical stability and poor adhesion to common inorganic substrates, both of which make it difficult to transfer their shape to the substrate. Traditional pattern transfer processes are based on the concept of *masking*, in which the mask protects the substrate from reacting with the harsh etchant. This approach requires that the mask be chemically and mechanically stable during the etching reaction. Molecular-scale templates such as DNA nanostructures are inherently incompatible with this pattern transfer approach. For example, two of the most often used methods to etch silicon oxide (SiO_2) are dry etching using plasma and wet etching using buffered HF solution. The plasma would instantly destroy the DNA, while the buffered HF solution would immediately lift the DNA off the substrate. Indeed, while DNA nanostructures have been used as templates for nanofabrication,[18,19] these processes have inevitably used an evaporated metal film as the intermediate etching mask. A one-step pattern transfer from DNA to an inorganic substrate has not been reported.

Herein we propose a new approach to pattern transfer in which the DNA modulates the vapor-phase etching of SiO_2 at the single-molecule level, resulting in a direct pattern transfer from DNA to SiO_2.

Vapor-phase etching has been known to produce selective, reproducible, and uniform etching of various inorganic substrates. Relative to the wet-etching and plasma-etching processes, it offers much more versatility in the range of process variables,[20,21] and most important of all, vapor-phase etching can be carried out under very mild conditions that will not lift off or destroy the DNA-based templates.

The vapor-phase etching of SiO_2 using HF gas is characterized by the thermodynamically favorable reaction between SiO_2 and HF gas to produce SiF_4 and H_2O:[21]

$$SiO_2(s) + 4HF(g) \rightarrow SiF_4(g) + 2H_2O(g)$$

However, to overcome the kinetic barrier, water is needed as a catalyst in the reaction, since HF alone does not etch SiO_2. Experimental evidence based on in situ FTIR spectroscopy has suggested that HF and H_2O molecules form a HF−H_2O complex that adsorbs on the SiO_2 surface more strongly than either molecule alone.[21,22] Other mechanistic studies[21] have suggested that the etching reaction starts with the deprotonation of HF by water to generate HF_2^- ions:

$$6HF + 3H_2O \rightarrow 3HF_2^- + 3H_3O^+$$

These ions then etch away SiO_2 to produce water and other gaseous products:

$$3HF_2^- + 3H_3O^+ + SiO_2 \rightarrow 2HF + SiF_4 + 5H_2O$$

The reaction is usually initiated by the trace amount of surface-adsorbed water on the oxide substrate. Notably, more water (5 equiv) is produced in the etching step than initially consumed (3 equiv) in the deprotonation step. As the reaction progresses, both the surface water concentration and the reaction rate increase; the overall reaction is autocatalytic.

All of this information suggests that the etching rate of SiO_2 is positively correlated with the concentration of surface-adsorbed water. We hypothesized that if the adsorption of water on the SiO_2 surface could be controlled with nanometer-scale resolution, it would be possible to modulate the etching of SiO_2 at the same length scale. The spatial variation in the concentration of surface-adsorbed water would not need to be very high: since the etching reaction is autocatalytic, small variations in the initial

Received: April 27, 2011

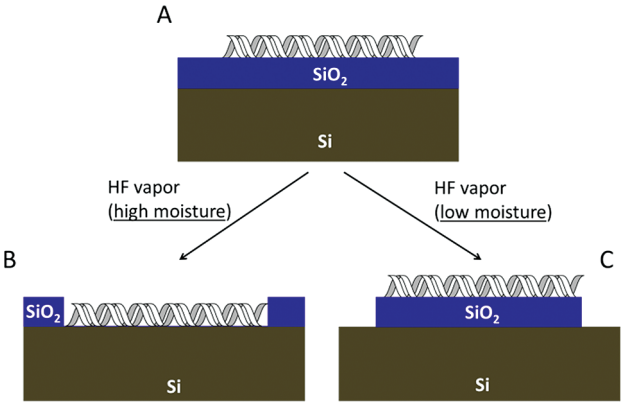

Figure 1. Pattern transfer from DNA to SiO_2. (A) Single strand of DNA deposited on the SiO_2 surface. (B) Negative tone pattern transfer through DNA-mediated etching of SiO_2. (C) Positive tone pattern transfer through DNA-mediated masking of SiO_2.

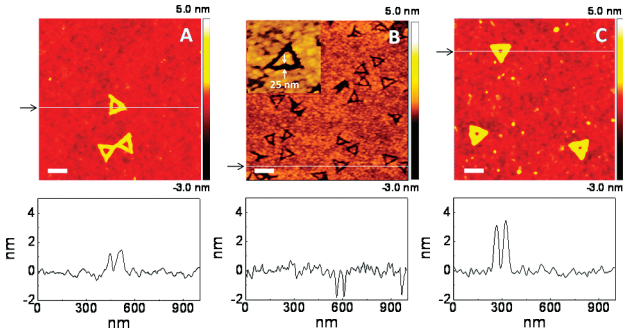

Figure 2. (top) AFM images and (bottom) cross sections: (A) Triangular DNA origami on a SiO_2 surface. (B) Triangular trenches produced upon exposure of (A) to HF vapor under high-moisture conditions. The inset shows a high-magnification AFM image of a triangular trench with a width of 25 nm. (C) Triangular ridges produced upon exposure of (A) to HF vapor under low-moisture conditions. Arrows indicate the lines along which the cross sections were determined. Scale bars represent 100 nm.

water concentration would be amplified by the reaction and could have a significant impact on the etching kinetics in the long run.

To verify this hypothesis experimentally, we used DNA nanostructures as templates for spatial modulation of the adsorption of water on a SiO_2 surface. DNA molecules contain phosphate groups as well as nitrogen and oxygen atoms that can hydrogen bond with water.[23] When a DNA molecule is deposited onto a SiO_2 surface, its presence undoubtedly affects the water adsorption around it. Since the SiO_2 surface also absorbs water by itself, the difference between the concentrations of surface-absorbed water on the clean SiO_2 surface and the SiO_2 under DNA depends on, among many other factors, the relative humidity of the environment and the temperature of the substrate. Though we cannot predict the exact spatial profile of the water concentration, we expect the DNA molecule to provide local modulation of the etching rate of SiO_2, producing nanoscale patterns that duplicate its shape.

There are two major differences between the water adsorption isotherms on DNA[23] and on SiO_2[24] at room temperature. First, the SiO_2 surface retains about a monolayer of water even at close to zero relative humidity; such irreversible adsorption is not observed on DNA. Second, DNA shows a much higher response to increases in relative humidity than SiO_2 does. Qualitatively speaking, the amount of adsorbed water on SiO_2 is higher at low humidity levels but lower at high humidity levels. On the basis of this analysis, we expect DNA to increase or decrease the etching rate of SiO_2 depending on the relative humidity of the environment (Figure 1).

We investigated the effect of DNA on the kinetics of gas-phase etching of SiO_2. We deposited triangular DNA origami onto a silicon wafer having a 300 nm layer of silicon oxide.[5,25] Figure 2A shows an atomic force microscopy (AFM) image of the deposited DNA origami. The etching of SiO_2 was carried out by exposing the substrate to HF gas inside a custom-built chamber that maintained ~50% relative humidity at 25 °C. After the etching, the silicon substrate was rinsed with water and piranha solution to remove the DNA. AFM images of the cleaned wafer surface showed triangular-shaped trenches resembling the shape of the DNA origami (Figure 2B and Figure S1 in the Supporting Information). The formation of the trench indicates that the DNA origami locally increases the rate of oxide etching under these conditions. The full width at half-maximum (fwhm) of the trench (16.7 ± 2.8 nm) is comparable with the edge width of the DNA origami, indicating an overall faithful pattern transfer process (Table S1 in the Supporting Information). This result is consistent with our hypothesis that DNA can increase the etching rate of SiO_2 by increasing the concentration of water. The small width of the trench shows that this effect is indeed spatially localized around the DNA.

As we pointed out earlier, the relative humidity may play an important role in this reaction. Indeed, we found that at low relative humidity, the DNA nanostructure slows the etching of the underlying SiO_2, resulting in a positive tone pattern transfer from the DNA to the substrate. As an example, the triangular DNA origami deposited on SiO_2 (Figure 2A), upon exposure to HF vapor at ~34% relative humidity and 30 °C, produced triangular ridges higher than the origami itself (Figure 2C and Figures S2 and S3). These ridge features survived a piranha wash and a heat treatment (600 °C in air for 15 min), indicating that they are not artifacts due to DNA or adsorbed organic impurities. As shown in the AFM cross sections in Figure 2, the height of the DNA origami triangle was ~1 nm (Figure 2A) while that of the resulting triangular feature obtained on SiO_2 was ~3 nm (Figure 2C). The width (fwhm) of the ridge was 27.0 ± 3.5 nm, which is much wider than that of the trench. We attribute this difference to the AFM tip convolution, which affects only the measurement of the ridges. Overall, our observations are consistent with the idea that at low humidity levels, clean SiO_2 is the preferred adsorption site for water. As a result, the autocatalytic etching of SiO_2 under the DNA is slower than that of the clean SiO_2 surface.

Once we had proved the concept, our next goal was to probe the resolution limit of this technique. For this purpose, we carried out the etching experiment with just a single double-stranded DNA as the template. To access individual DNA molecules, we aligned λ-DNA on the SiO_2 substrate using a previously published procedure.[26] λ-DNA is a double-stranded phage DNA with a length of ~16 μm when fully stretched. Figure 3A shows an AFM image of the DNA strands on the SiO_2 surface. The height of the DNA molecules was in the range 0.6−0.7 nm, consistent with the diameter of a single strand of λ-DNA. Bundling of the DNA, however, was evident in many of the

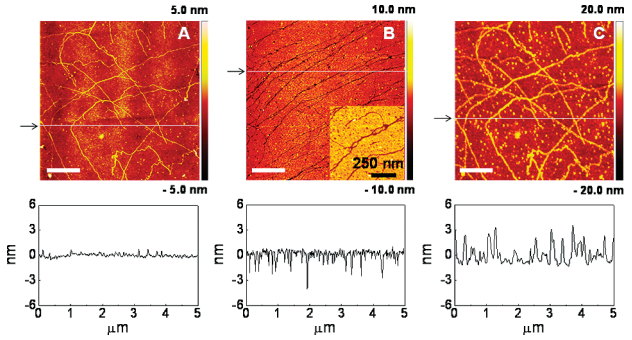

Figure 3. (top) AFM images and (bottom) cross sections: (A) λ-DNA aligned on the SiO_2 substrate. (B) Trenches produced after exposure of (A) to HF vapor under high-moisture conditions. The inset shows a high-magnification image of the trench. (C) Ridges produced after exposure of (A) to HF vapor under low-moisture conditions. It should be noted that this AFM image was obtained at exactly the same location as the one in (A). Arrows indicate lines along which the cross sections were determined. Scale bars represent 1 μm.

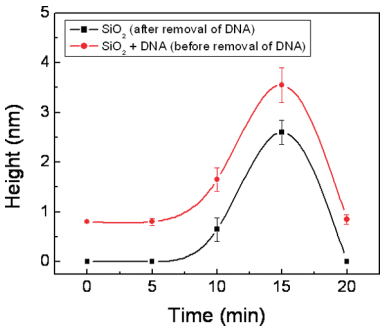

Figure 4. Temporal evolution of the height of the ridges obtained under low-moisture conditions. Measurements were carried out before (SiO_2 + DNA; black) and after (SiO_2 only; red) cleaning of the surface.

strands. After the etching under high-moisture conditions (~50% relative humidity), long trenches were observed on the SiO_2 surface (Figure 3B). The width of the trenches was measured to be 23.5 ± 4.2 nm (Figure S4 and Table S1) though trenches with widths of less than 10 nm were located (Figure S5). We believe that the bundled DNA strands produced the wide trenches while the narrower ones were formed by the single DNA strands.

The etching experiment with the stretched λ-DNA was also carried out under low-moisture conditions (~34% relative humidity). It was observed that even a single strand of λ-DNA can slow the etching of SiO_2 underneath it. In one experiment, we imaged the exact same location before (Figure 3A) and after the etching (Figure 3C). The height of the ridge features after the etching was 2−4 nm, representing a 3−6× amplification of the height of the DNA template. More importantly, we observed a very faithful pattern transfer from the DNA template to the SiO_2 substrate.

Our proposed mechanism is supported by a kinetics study of the etching reaction under the low-moisture conditions (Figure 4). SiO_2 substrates with aligned λ-DNA on the surface were etched for 5, 10, 15, and 20 min and imaged using tapping-mode AFM before and after the cleaning (piranha/heat-treatment) process. The difference in the two measurements (~0.7 nm) indicates the presence of the DNA template throughout the reaction. An induction period (~5 min) was observed, and this was followed by a rapid buildup of the ridge height, signifying the autocatalytic nature of the reaction.[21] At longer reaction times, however, enough water was produced by the reaction to saturate the surface, leading to an eventual decrease in the contrast. The substrate temperature also plays a significant role in determining the etching kinetics. We observed that the etching rate decreased with increasing substrate temperature, likely as a result of the decrease in water adsorption on the SiO_2 surface. This observation further confirms our working hypothesis that the pattern transfer from DNA to SiO_2 substrate is due to the spatial variation in the concentration of surface-adsorbed water.

In conclusion, we have demonstrated a new approach to pattern transfer from DNA to SiO_2. DNA was used to increase or decrease the etching rate of SiO_2, resulting in negative or positive tone pattern transfers to the substrate, respectively. Our still unoptimized conditions routinely produce 20 nm wide trenches, which may be useful as nanofluidic channels.[27,28] This method, if applied to a much thinner SiO_2 film, would produce a patterned SiO_2 layer that could be used as a mask for etching of the underlying silicon substrate. We believe that this methodology will open up new opportunities in using self-assembled soft materials as templates for bottom-up nanofabrication, with the possibility of achieving molecular-scale resolution.

■ ASSOCIATED CONTENT

Supporting Information. Experimental details, additional figures, and a table. This material is available free of charge via the Internet at http://pubs.acs.org.

■ AUTHOR INFORMATION

Corresponding Author
hliu@pitt.edu

Author Contributions
[§]These authors contributed equally.

■ ACKNOWLEDGMENT

Financial support from the University of Pittsburgh is acknowledged. We thank Keith Jones of Asylum Research for acquiring some of the AFM images.

■ REFERENCES

(1) http://www.itrs.net/Links/2007ITRS/Home2007.htm (accessed April 2011).
(2) Seeman, N. C. *Annu. Rev. Biochem.* **2010**, *79*, 65–87.
(3) Hung, A. M.; Noh, H.; Cha, J. N. *Nanoscale* **2010**, *2*, 2530–2537.
(4) Voigt, N. V.; Tørring, T.; Rotaru, A.; Jacobsen, M. F.; Ravnsbæk, J. B.; Subramani, R.; Mamdouh, W.; Kjems, J.; Mokhir, A.; Besenbacher, F.; Gothelf, K. V. *Nat. Nanotechnol.* **2010**, *5*, 200–203.
(5) Hung, A. M.; Micheel, C. M.; Bozano, L. D.; Osterbur, L. W.; Wallraff, G. M.; Cha, J. N. *Nat. Nanotechnol.* **2010**, *5*, 121–126.
(6) Sharma, J.; Chhabra, R.; Cheng, A.; Brownell, J.; Liu, Y.; Yan, H. *Science* **2009**, *323*, 112–116.
(7) Maune, H. T.; Han, S.-p.; Barish, R. D.; Bockrath, M.; Goddard, W. A., III; Rothemund, P. W. K.; Winfree, E. *Nat. Nanotechnol.* **2010**, *5*, 61–66.
(8) Zhang, J.; Liu, Y.; Ke, Y.; Yan, H. *Nano Lett.* **2006**, *6*, 248–251.
(9) Keren, K.; Berman, R. S.; Buchstab, E.; Sivan, U.; Braun, E. *Science* **2003**, *302*, 1380–1382.

(10) Ding, B.; Deng, Z.; Yan, H.; Cabrini, S.; Zuckermann, R. N.; Bokor, J. *J. Am. Chem. Soc.* **2010**, *132*, 3248–3249.
(11) Xin, H.; Woolley, A. T. *J. Am. Chem. Soc.* **2003**, *125*, 8710–8711.
(12) Pal, S.; Deng, Z.; Ding, B.; Yan, H.; Liu, Y. *Angew. Chem., Int. Ed.* **2010**, *49*, 2700–2704.
(13) Yan, H.; Park, S. H.; Finkelstein, G.; Reif, J. H.; LaBean, T. H. *Science* **2003**, *301*, 1882–1884.
(14) Ding, B.; Wu, H.; Xu, W.; Zhao, Z.; Liu, Y.; Yu, H.; Yan, H. *Nano Lett.* **2010**, *10*, 5065–5069.
(15) He, Y.; Chen, Y.; Liu, H.; Ribbe, A. E.; Mao, C. *J. Am. Chem. Soc.* **2005**, *127*, 12202–12203.
(16) Kershner, R. J.; Bozano, L. D.; Micheel, C. M.; Hung, A. M.; Fornof, A. R.; Cha, J. N.; Rettner, C. T.; Bersani, M.; Frommer, J.; Rothemund, P. W. K.; Wallraff, G. M. *Nat. Nanotechnol.* **2009**, *4*, 557–561.
(17) Gerdon, A. E.; Oh, S. S.; Hsieh, K.; Ke, Y.; Yan, H.; Soh, H. T. *Small* **2009**, *5*, 1942–1946.
(18) Becerril, H. A.; Woolley, A. T. *Small* **2007**, *3*, 1534–1538.
(19) Deng, Z.; Mao, C. *Angew. Chem., Int. Ed.* **2004**, *43*, 4068–4070.
(20) Lee, Y.-I.; Park, K.-H.; Lee, J.; Lee, C.-S.; Yoo, H. J.; Kim, C.-J.; Yoon, Y.-S. *J. Microelectromech. Syst.* **1997**, *6*, 226–233.
(21) *Handbook of Silicon Wafer Cleaning Technology*, 2nd ed.; Reinhardt, K. A., Kern, W., Eds.; William Andrew: Norwich, NY, 2008; pp 281−304.
(22) Montano-Miranda, G.; Muscat, A. J. *Diffus. Defect Data, Pt. B* **2003**, *92*, 207–210.
(23) Balkose, D.; Alp, B.; Ulku, S. *J. Therm. Anal. Calorim.* **2008**, *94*, 695–698.
(24) Mizushima, S. *Metrologia* **2004**, *41*, 137–144.
(25) Please see the Supporting Information for experimental details.
(26) Deng, Z.; Mao, C. *Nano Lett.* **2003**, *3*, 1545–1548.
(27) Xia, Q. F.; Morton, K. J.; Austin, R. H.; Chou, S. Y. *Nano Lett.* **2008**, *8*, 3830–3833.
(28) Nam, S.-K.; Lee, M.-H.; Lee, S.-H.; Lee, D.-J.; Rossnagel, S. M.; Kim, K.-B. *Nano Lett.* **2010**, *10*, 3324–3329.